

Deliverable 5.2: Growth of catalyst-free Hex-SiGe substrate.

Task 5.1. (TU/e, JKU) “Fabrication of a Hex-SiGe substrate”. We will develop a scheme to grow a (Au-free) Hex-SiGe layer on a conventional silicon substrate. We will use selective area growth of WZ GaP, which will be used to grow Hex-Si shell. Removal of the GaP by selective etching and further Si growth will result in a dense Hex-Si layer. Strain and defect density will be studied by XRD techniques. **This is milestone 7 (M24).**

Task 5.2. (IBM, JKU) “Wurtzite virtual substrates as templates for Hex-Si(Ge)”. Templates for micron-sized virtual substrates will be developed and growth conditions for pure wurtzite GaP using TASE will be determined based on learnings from Task 4.1. Both vertical and horizontal structures will be explored.

D5.1 Progress on CMOS compatibility. [M18]

D5.2 Growth of catalyst-free Hex-SiGe substrate. [M24]

D5.3 Report on CMOS compatible Hex-SiGe layers. [M48]

We are employing Template-Assisted Selective Epitaxy (TASE) to grow III-V materials without the use of a (Au-) catalyst. This method has previously been used at IBM to integrate high quality material with very well-defined geometry for electrical and optical devices, however complete phase-transitions have not been observed before with this technique. Such a transition would allow for planar virtual WZ substrates that could be used to grow catalyst-free Hex-SiGe layers.

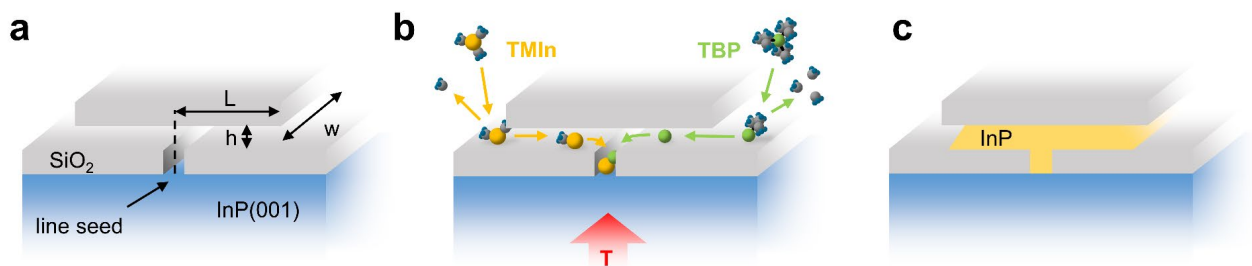


Figure 1. TASE of large-area InP. (a) Empty SiO₂ cavity as processed on top of an InP(001) substrate. The template can be extended arbitrarily wide in the out-of-plane direction (w). (b) Sketch of the selective epitaxy process. (c) Template after MOCVD growth.

To address this, we previously (Deliverable 5.1) studied the (catalyst-free) Selective Area Growth (SAG) of III-V materials and were able to find growth conditions to form pure WZ InP Nanowires. In order to obtain planar large-area films we shifted our effort towards TASE on InP(001) substrates, as schematically shown in Figure 1. Due to the confined nature of TASE, we expect differences in the growth dynamics with respect to SAG. Most importantly it should be noted that the growth direction can be designed along different crystallographic orientations, which is important since phase transitions are only expected to be formed along the ZB $\langle 111 \rangle$ direction. We have studied two growth orientations perpendicular to the (001) wafer orientation: $\langle 100 \rangle$ and $\langle 110 \rangle$. As illustrated in Figure 2, only the latter allows for $\{111\}$ facets and therefore for planar defects (PDs) to be formed to facilitate a ZB-WZ phase transition.

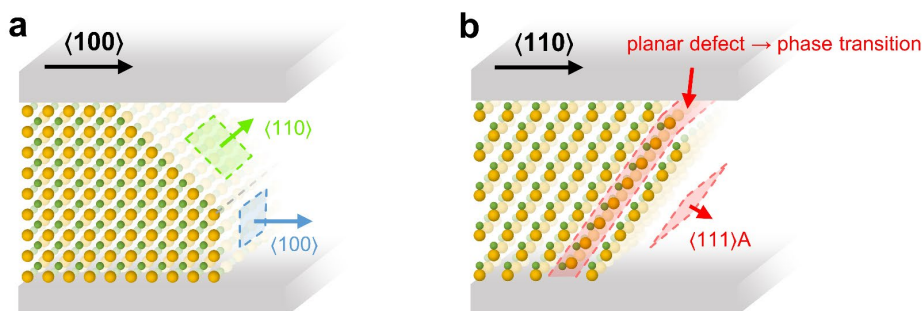


Figure 2. Illustrations to show faceting along (a) $\langle 100 \rangle$ and (b) $\langle 110 \rangle$ growth directions. $\{111\}$ facets and therefore PDs can only be formed in the latter case.

We employ standard InP growth conditions in our MOCVD reactor ($V/III = 100$, $T=550C$) to demonstrate this principle. Figure 3 shows a representative InP layer grown along $\langle 100 \rangle$ direction. No PDs can be found and thus pure ZB InP is obtained as expected due to the lack of $\{111\}$ facets during the growth. On the other hand, a typical InP layer grown along the $\langle 110 \rangle$ direction during the same growth run is shown in Figure 4. We observe pure ZB material without PDs for the first few tens of nanometers (Figure 4c), which is due to the absence of $\{111\}$ facets at the beginning of the growth. However, as soon as the $(111)A$ facet forms out, we immediately obtain a high density of PDs (~ 1 PD/nm), as it is depicted in more detail in Figure 4d. In addition to the two possible stacking orientations (ABC, CBA) of ZB we see short segments of WZ already, which corresponds to the uncolored regions.

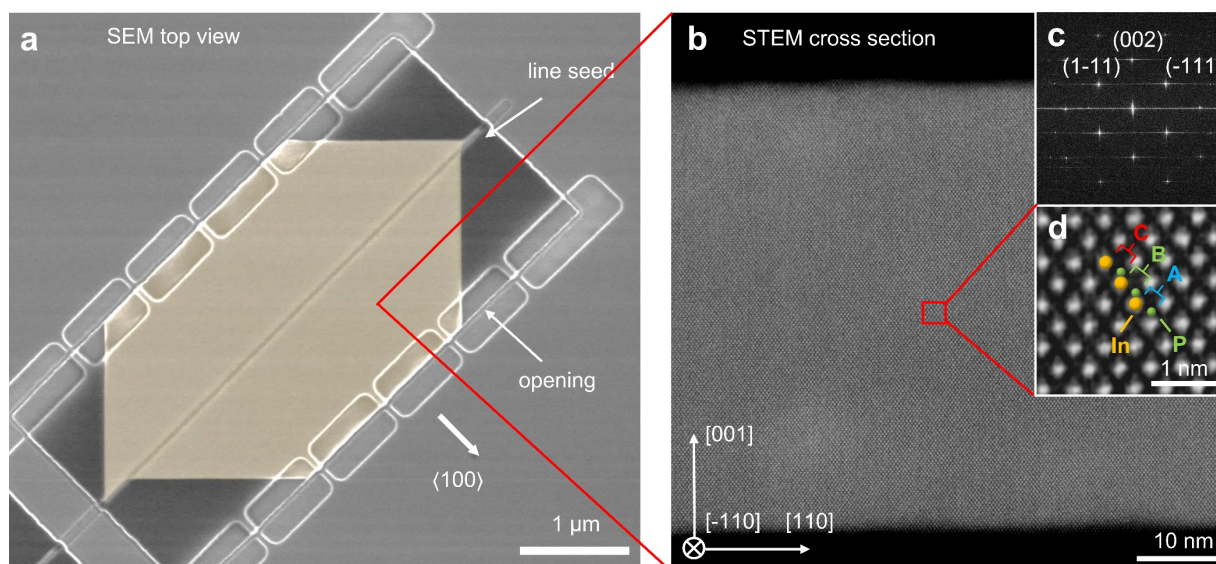


Figure 3. InP layer grown along $\langle 100 \rangle$ at 550C. (a) SEM top view image showing clear and defined faceting. The crystal expands from the central line seed towards the openings. (b) Representative STEM cross section of such a film viewed along $[-110]$ zone axis. No planar defects are found. (c) Corresponding FFT pattern showing ZB symmetry. (d) HR-image demonstrating the ABC type stacking.

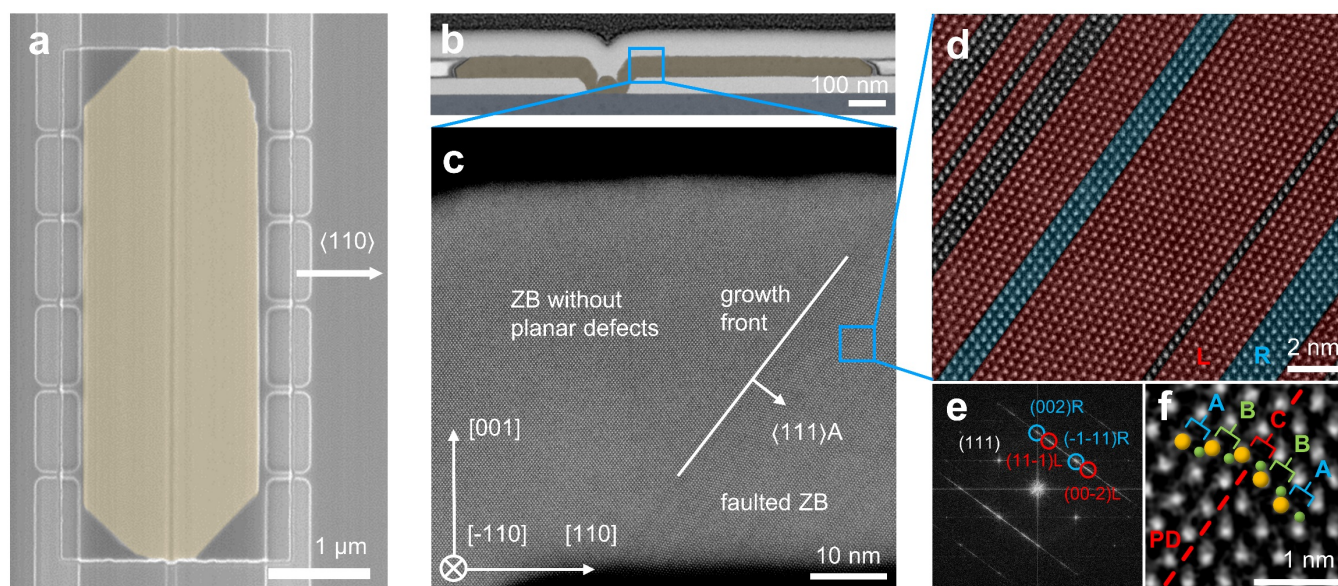


Figure 4. InP layer grown along $\langle 110 \rangle$ at 550C. (a) SEM top view image. (b) Corresponding cross section STEM image from a different crystal viewed along $[-110]$ zone axis. (c) Close-up STEM micrograph close to the nucleation point. (d) HR-STEM image. Colored areas represent ZB segments with the two possible stacking orientations (ABC, CBA). (e) Corresponding FFT pattern showing faulted ZB symmetry. (f) Detailed micrograph of the crystal stacking.

From earlier SAG experiments we know that increasing the growth temperature promotes the formation of WZ phase in InP nanowires. We therefore performed a growth series of InP sheets at various temperatures, to find the optimal conditions. Figure 5a summarizes our experiments. The number of twinned bilayers in $\langle 110 \rangle$ grown crystals gradually increases, when the growth temperature is increased from 550C to 650C, while InP grown along $\langle 100 \rangle$ stays defect-free. 100% twinning in this plot corresponds to pure WZ material. At 650C we could reach 97% as it is more detailed in Figure 5b-d. This was achieved by ramping up the growth temperature from 600C during the first 5 min to prevent desorption of the otherwise unstable InP(001) surface. Increasing the temperature further is expected to result in even higher phase purity, however the TBP pressure in our MOCVD reactor was not sufficient to stabilize the InP surface under such conditions. Figure 5e demonstrates the optical quality of the grown films and serves as an additional proof for the phase change obtained. It is worth mentioning that this is the first report of large area planar WZ films in a material that naturally crystallizes in ZB symmetry. These results were published recently¹.

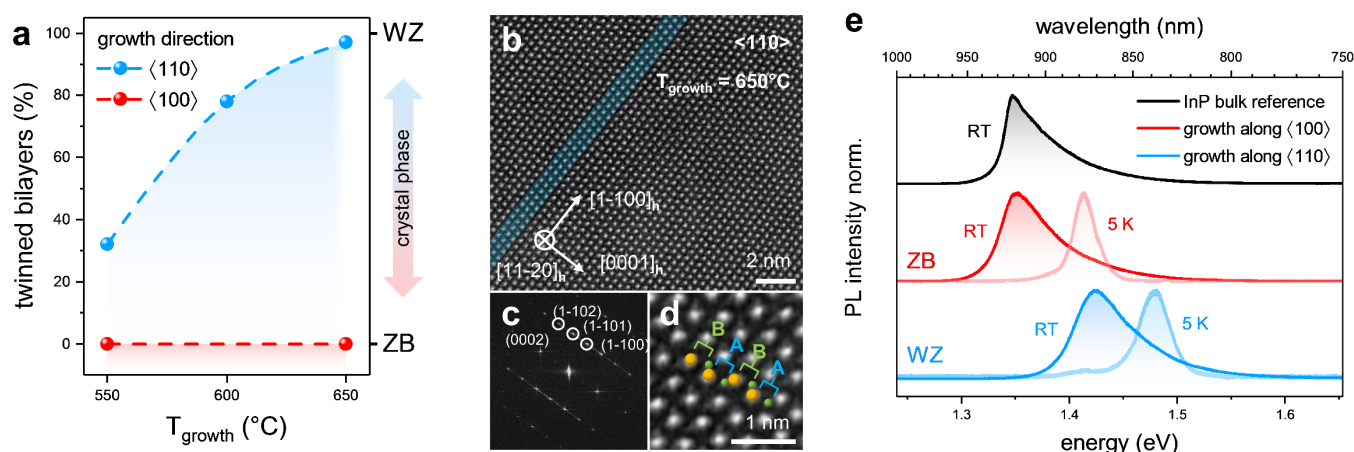


Figure 5. Simultaneous growth of ZB and WZ InP layers. (a) Number of twinned bilayers as a function of growth temperature for InP films grown along $\langle 110 \rangle$ and $\langle 100 \rangle$. (b) STEM investigation of an InP crystal grown along $\langle 110 \rangle$ at 650C. All uncolored regions are pure WZ. (c) Corresponding FFT pattern showing WZ symmetry. (d) HR-image demonstrating the ABAB type stacking. (e) Normalized PL emission spectra of typical crystals along with bulk InP(001) at RT as well as 5 K.

In summary, we have achieved control over the formation of the crystal phase of large area planar InP films and can tune from pure ZB to WZ. Next step will be to transfer the crystal structure along the vertical direction to SiGe. Since the lattice constant of InP is relatively far from both Si and Ge, we expect high amounts of defects in such an epitaxy. We therefore work in parallel on the growth of WZ GaAs and other lattice matched materials.

Progress on Hex-Ge substrates

We have grown Ge shells around a square pattern of Wurtzite (WZ) GaAs cores with 50nm diameter, 2.5 μ m length and 1 μ m pitch, following the recipe developed in workpackage 1. The shell growth is continued up to the point in which the shells grown around different cores touch each other and merge into a single substrate-like structure. The concept and SEM images of the resulting crystal are illustrated in Fig 6.

As shown in Fig. 6a, the Ge grows around the cores forming the hexagonal phase. It grows as well on their top and on the substrate, forming the cubic phase.

¹ Staudinger, P., Mauthe, S., Moselund, K. E., Schmid, H. "Concurrent Zinc-Blende and Wurtzite Film Formation by Selection of Confined Growth Planes." Nano Lett. **2018**, 18 (12), 7856-7862

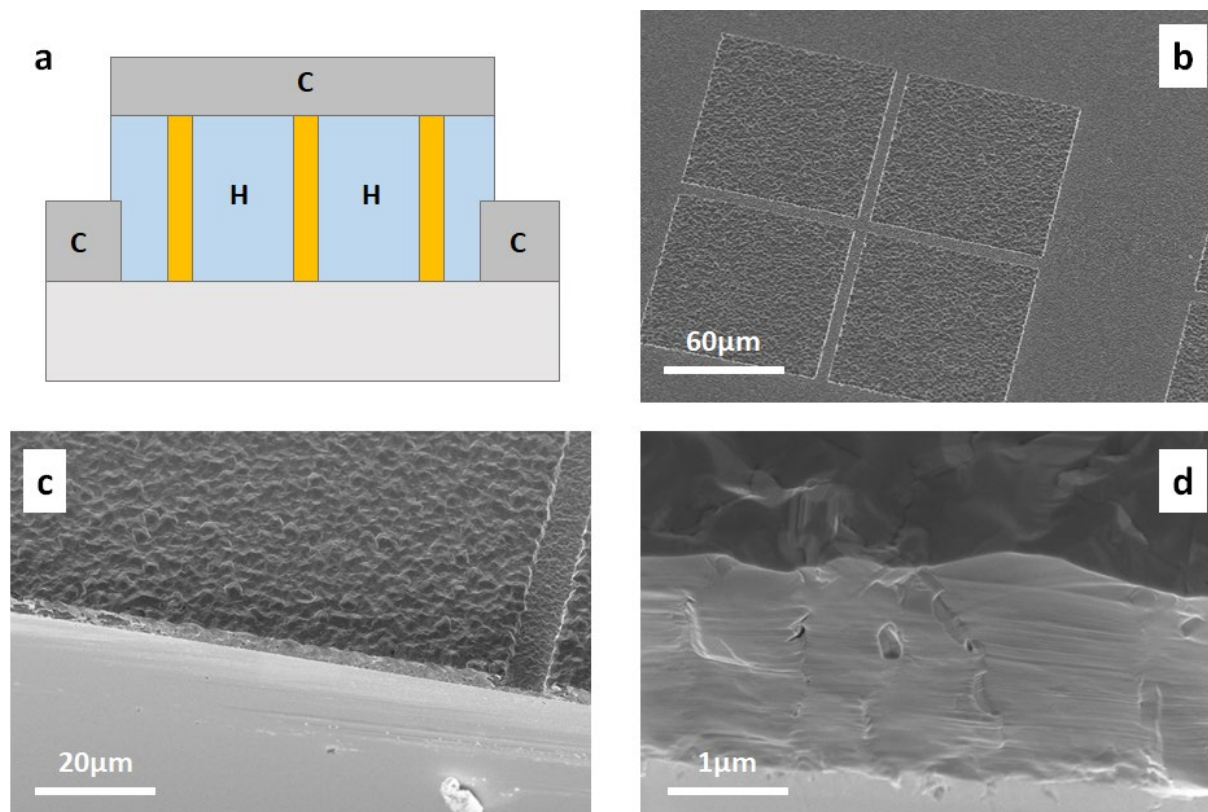


Figure 6: a) Schematic of the hex-Ge substrate growth method. Yellow: Wurtzite GaAs nanowires. H: hexagonal Germanium. C: cubic Germanium. Substrate: Zincblende GaAs. b-d) SEM images of a hex-Ge substrate at different magnifications. In c-d) the sample was cleaved in order to obtain a cross-sectional SEM image of the Ge crystal.

In order to assess the crystal structure of Ge, we use Focused Ion Beam (FIB) to cut a lamella of 100nm in thickness from within the structure, so to make Transmission Electron Microscopy (TEM) analysis possible. Bright field TEM images of the lamella are shown in Fig. 7.

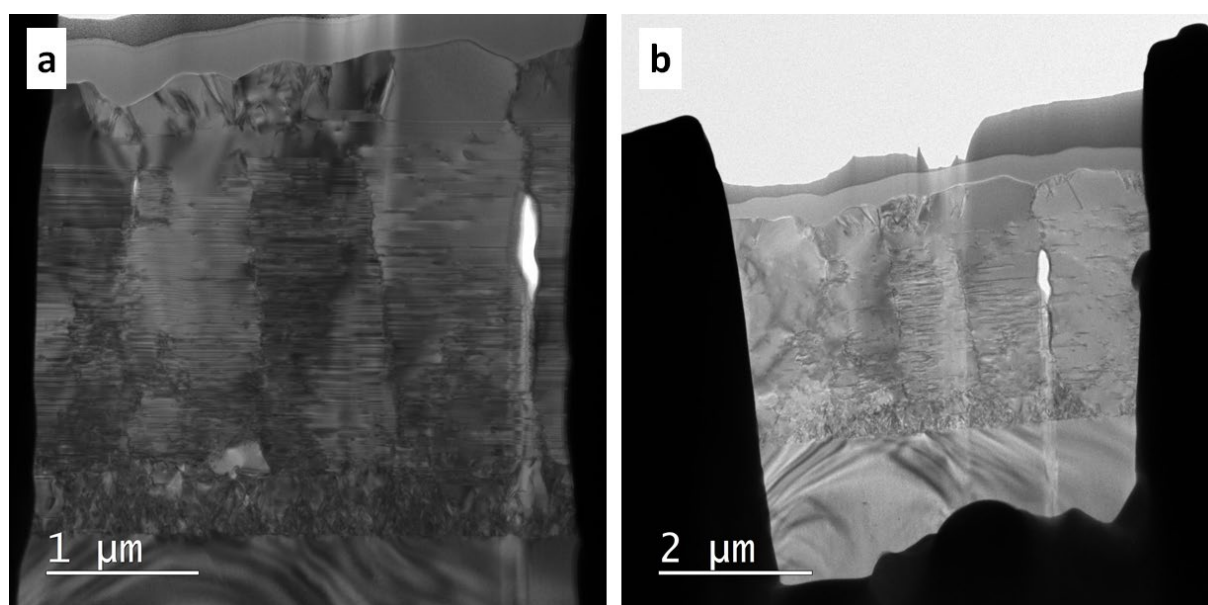


Figure 7: TEM bright field images of the Ge lamella, imaged in the a) $\langle 10-10 \rangle$ zone axis and b) $\langle 11-20 \rangle$ zone axis.

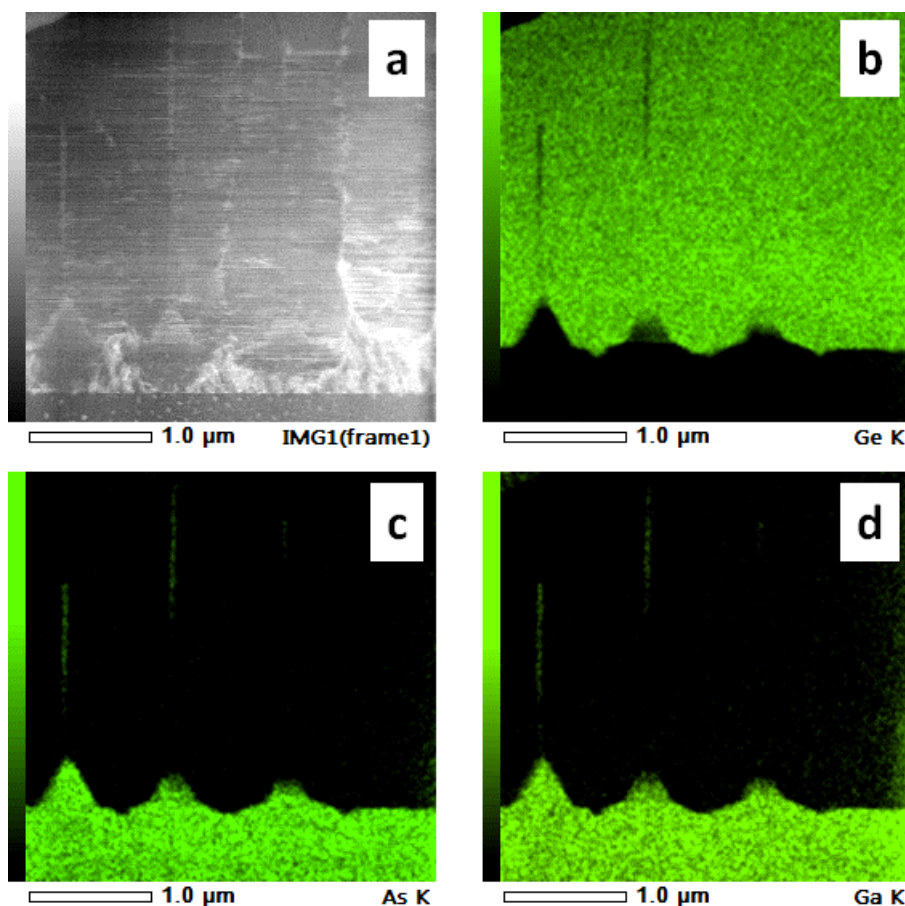


Figure 8: EDX analysis of a section of the Ge lamella. a) HAADF image. b-d) EDX 2D maps of the b) Ge, c) As and d) Ga signals. Two thin GaAs cores are visible, as well as their pedestals grown on the substrate.

In Fig. 8 we show the EDX analysis of a section of the lamella, revealing the presence of the GaAs cores in the Ge substrate-like structure.

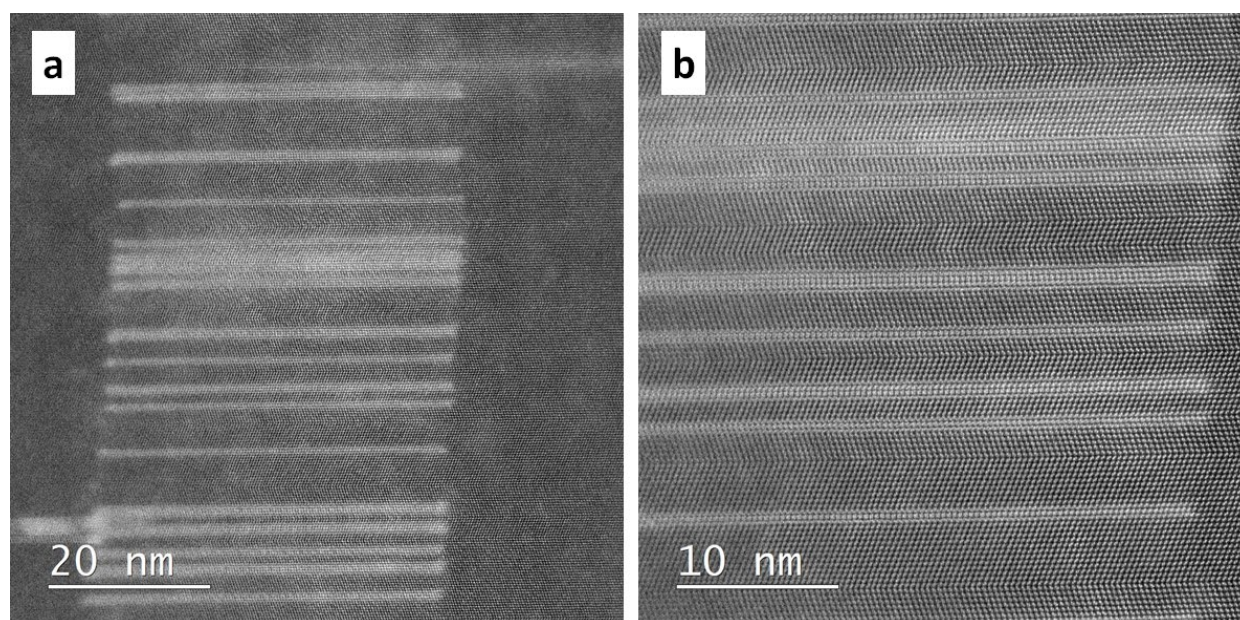


Figure 9: HR-STEM image of a GaAs nanowire embedded in the Ge continuous film. In b) we can see the crystal structure of both the GaAs nanowire and the Ge, being cubic.

We investigated the crystal structure of the cores and Ge crystal with High Resolution Scanning TEM (HR-STEM) as shown in Fig. 9. The crystal structure is found to be cubic with numerous twins, both for the GaAs cores and the Ge layer. However, TEM analysis of the freestanding cores before Ge growth yielded pure WZ phase.

We therefore conclude that the original phase of the GaAs cores was WZ, as well as the phase of the initial Ge epilayer. When the Ge shells touched, the resulting pressure forced the WZ GaAs crystal cores to switch to the cubic structure, as observed in previous cases reported in literature^{2,3}.

In the future Ge shells might be grown for a shorter time in order to stop the growth at the moment in which the shells touch, thus limiting the time available for the crystal to revert to cubic structure.

Ge shells might be grown for long times around isolated WZ GaAs cores, in order to obtain shells with very large diameter ($>10\mu\text{m}$) with substrate-like dimension.

Larger WZ GaAs structures can also be envisioned, such as WZ GaAs walls, from which large crystals of hexagonal Ge can be epitaxially grown.

² Jacobsson et al. Cryst. Growth Des. 2015, 15, 4795–4803

³ G. Patriarche, Nano Lett. 8, 1638 (2008)